


Assembly and Purification of Polyomavirus-Like Particles from Plants

Emeline V. B. Catrice¹ · Frank Sainsbury¹ 

Published online: 16 July 2015

© Springer Science+Business Media New York 2015

Abstract Polyomaviruses are small DNA viruses that have a history of use in biotechnology. The capsids of a number of species have been developed into experimental prophylactic and therapeutic virus-like particle (VLP) vaccines. In order to explore plants as a host for the expression and purification of polyomavirus-like particles, we have transiently expressed the major capsid protein, VP1, in *Nicotiana benthamiana* leaves. Deletion of a polybasic motif from the N-terminal region of VP1 resulted in increased expression as well as reduced necrosis of leaf tissue, which was associated with differences in subcellular localisation and reduced DNA binding by the deletion variant (Δ VP1). Self-assembled VLPs were recovered from tissue expressing both wild-type VP1 and Δ VP1 by density gradient ultracentrifugation. VLPs composed of Δ VP1 were more homogenous than wtVLPs and, unlike the latter, did not encapsidate nucleic acid. Such homogenous, empty VLPs are of great interest in biotechnology and nanotechnology. In addition, we show that both MPyV VLP variants assembled in plants can be produced with encapsidated foreign protein. Thus, this study demonstrates the utility of plant-based expression of polyomavirus-like particles and the suitability of this host for further developments in polyomavirus-based technologies.

Keywords Virus-like particle · Recombinant protein · Molecular farming · Transient expression · Vaccine

Abbreviations

AF4	Asymmetric flow field-flow fractionation
DLS	Dynamic light scattering
Dpi	Days post-infiltration
GFP	Green fluorescent protein
NLS	Nuclear localisation signal
PBS	Phosphate-buffered saline
TEM	Transmission electron microscopy
VLP	Virus-like particle
wt	Wild-type

Introduction

Polyomaviruses are small double-stranded DNA viruses of the family *Polyomaviridae*. The single genus comprises at least 32 species infecting mammals and birds including the type species, *Simian virus 40*, the well-studied *Murine polyomavirus* (MPyV) and the cancer-causing *Merkel cell polyomavirus* (MCPyV). Polyomavirus capsids are non-enveloped icosahedra approximately 45 nm in diameter, composed of 72 pentameric capsomeres of the major coat protein, VP1, arranged with $T = 7d$ symmetry. Self-assembling virus-like particles (VLPs) can be generated from overexpressed VP1 in eukaryotic cells [40] or from isolated capsomeres in vitro [37]. These particles have found many uses in biotechnology, from vaccines to the delivery of various cargos such as nucleic acid, proteins and small molecules [46].

VLPs can be used as immunogens to direct immune responses against their cognate virus or as carriers of

Electronic supplementary material The online version of this article (doi:10.1007/s12033-015-9879-9) contains supplementary material, which is available to authorised users.

✉ Frank Sainsbury
f.sainsbury@uq.edu.au

¹ Centre for Biomolecular Engineering, Australian Institute for Bioengineering and Nanotechnology (AIBN), The University of Queensland, St Lucia, QLD 4072, Australia

epitopes from other disease-causing agents [20]. With recent expansion of the human polyomavirus family and the association of polyomaviruses with potentially fatal pathologies in immunocompromised patients, there is renewed interest in vaccine development [12, 29, 49]. In addition, MPyV in particular has been developed as a carrier of heterologous epitopes and proteins [1, 25, 41] for the prevention of heterologous infectious diseases, of both viral [3] and bacterial [32] origin, and as therapeutic cancer vaccines [45]. The latter application takes advantage of the addressable interior of polyomavirus VLPs that permits the encapsidation of molecules fused or chemically conjugated to the minor coat protein, VP2 [1].

Concomitant with the development of biomedical applications for polyomavirus-like particles has been the development of expression strategies and bioprocesses for their production and formulation. Recombinant VP1 was first expressed in prokaryotes [18] where it is generally, though not exclusively, recovered as capsomeres for in vitro VLP assembly [37]. Subsequently, yeast, insect cells and mammalian cells have all been used as production hosts with varying outcomes [46]. While yeast cells have been successfully used to express VLPs with negligible DNA contamination [39], insect cell-derived VLPs, which contain relatively high levels of encapsidated DNA, have enabled facile co-expression of VP2 fusions, resulting in encapsidation of the fused protein, for biotechnology applications [6, 45].

Plant-based expression systems have developed into promising platforms for the production of VLPs [8, 42]. In addition, recent developments in transient expression methods have delivered scalable processes with commercially viable yields [30] as well as easy co-expression of multiple proteins [35]. The present study demonstrates that this approach can be used to express and recover polyomavirus VLPs from leaves of *Nicotiana benthamiana*. Removal of a polybasic N-terminal region of VP1 known to confer DNA binding and contribute to the nuclear localisation signal (NLS) resulted in increased VP1 expression, altered subcellular localisation and reduced leaf tissue necrosis. Characterisation of the VLPs assembled from both wtVP1 and the deletion variant showed that the variant generated VLPs that were more homogenous and, unlike wtVLPs, did not encapsidate DNA.

Materials and Methods

Cloning

The sequence encoding wild-type (wt) VP1 from MPyV (M34958) was amplified from a plasmid provided by Professor Robert Garcea (University of Colorado, CO, USA).

A codon-optimised (c.o.) version of VP1 was ordered from the GeneArt web portal (www.lifetechnologies.com) with *N. benthamiana* selected as the expression host. A synthetic gene encoding amino acids 251–301 of MPyV VP2 (nt 4251–4102 of NC_001515), fused to the N-terminus of enhanced green fluorescent protein (GFP; nt 675–1391 of U57609) via a duplicated Gly₄Ser linker, was also ordered via the GeneArt web portal. PCR primers incorporating overlapping sequences homologous to the expression plasmid, pEAQ-HT [36] (GQ497234), were designed with Geneious R7.1 software (Biomatters Ltd., www.geneious.com) and deletions in the N-terminal region of the translated protein were generated by omitting corresponding codons from the upstream primer. See supplementary materials for a table listing all primers used in this work. Restriction enzyme digest with *Age*I and *Stu*I was used to linearise pEAQ-HT, and expression constructs were assembled using the Gibson Assembly Master Mix (New England Biolabs, www.neb.com) according to the manufacturer's instructions. Recombinant plasmids were verified by Sanger sequencing.

Agrobacteria and Plant Transformation

Expression vectors were maintained *Agrobacterium tumefaciens* strain LBA4404, which was transformed by electroporation. Bacterial cultures were grown to stable phase in Luria–Bertani medium supplemented with kanamycin (50 µg/mL), streptomycin (50 µg/mL) and rifampicin (50 µg/mL) at 28 °C and 220 rpm. The cultures were gently pelleted at 2220 g for 22 min at 22 °C and resuspended in infiltration medium (10 mM MES (2-[*N*-morpholino]ethanesulphonic acid), pH 5.6, 10 mM MgCl₂, 100 µM acetosyringone) to an OD₆₀₀ of 0.4 and incubated for 3–4 h at ambient temperature. Agrobacteria suspensions were pressure-infiltrated with a needleless syringe into the underside of the leaves of 7-week-old *N. benthamiana* plants. For co-expression experiments, suspensions were mixed as described in the relevant section prior to infiltration.

Protein Extraction and Western Blotting

To minimise the variability of protein expression levels from leaves of different ages [33], the experiments were conducted to allow sampling from at least three different leaves per construct. Infiltrated leaf tissue was harvested as leaf discs equivalent to 120 mg of control-infiltrated tissue, and homogenised by disrupting tissue with 7-mm tungsten beads using a TissueLyserII (Qiagen, www.qiagen.com) with pre-chilled tube holders in three volumes of phosphate-buffered saline (PBS), pH 7.3, containing 5 mM ethylenediaminetetra-acetic acid (EDTA), 0.05 % (v/v) Triton X-100, and

complete protease inhibitor cocktail (Roche, www.roche.com). After incubating on ice for 5 min, the lysate was then clarified by centrifugation at 20,000g for 5 min at 4 °C, and the supernatant was transferred in a new tube. The concentrations of leaf extracts were determined using the microplate Bradford Assay (ThermoScientific, www.thermofisher.com) with BSA as the standard.

Protein extracts (10 µL) containing VP1 were resolved by SDS-PAGE under reducing conditions. Gels were stained with Coomassie Brilliant Blue G or electroblotted onto Amersham nitrocellulose membrane (GE Life Sciences, www.gelifesciences.com). Non-specific binding sites were blocked using 5 % (w/v) skim milk powder in PBS, containing 0.05 % (v/v) Tween-20, which also served as antibody dilution buffer. Anti-VP1 sera raised in mouse were applied at a 1 in 500 dilution followed by horseradish peroxidase (HRP)-conjugated goat anti-mouse IgG antibody (Sigma-Aldrich, www.sigmaaldrich.com), diluted 1 in 5000. Alternately, mouse anti-GFP (Cell Signalling Technologies, www.cellsignal.com) was applied at a 1 in 800 dilution, followed by the same HRP-conjugated secondary antibody. Chemiluminescent signal was obtained using the Clarity Western ECL Substrate (Bio-Rad, www.bio-rad.com).

VLP Purification

Large-scale extraction for VLP purification was performed on 8 g of whole infiltrated leaves with the mid vein removed. Tissue was disrupted using a PT1200 Polytron (www.kinematica.ch) at 25,000 rpm for 2 × 45 s in 3 volumes of cold extraction buffer (50 mM MOPS (3-morpholinopropane-1-sulfonic acid), pH 7.0, 0.5 M NaCl, 1 mM dithiothreitol (DTT), 0.01 % (v/v) Tween-80) containing 1 % (w/v) polyvinylpyrrolidone (PVPP) and complete protease inhibitor. After 10 min incubation on ice, cell debris was removed by passing the lysate through two layers of Miracloth (Merck-Millipore, www.emdmillipore.com). The filtered sample was then centrifuged at 18,000g for 10 min at 4 °C, and the supernatant was transferred to a new tube. An iodixanol density gradient was prepared using Optiprep (Sigma-Aldrich), a 60 % (w/v) solution of iodixanol in water. Solutions of 50, 40, 30 and 20 % iodixanol were prepared in 20 mM MOPS, pH 7.0, with 200 mM NaCl and 1 mM CaCl₂. Polyclear ultracentrifuge tubes (www.setonscientific.com) were prepared with 3 mL of each iodixanol density, which were then overlaid by 23 mL of clarified lysate. Tubes were placed in a Sorvall Surespin 630/36 rotor and centrifuged at 25,000 rpm for 3 h at 8 °C.

Fractions of 1 mL were collected by piercing the bottom of the tube and analysed by SDS-PAGE and Coomassie staining. Those fractions determined to contain VLPs were subject to buffer exchange using PD MidiTrap G-25

desalting columns (GE Life Sciences) with 20 mM Tris-base, pH 7.4, containing 200 mM NaCl, 1 mM CaCl₂ and 5 % (v/v) glycerol. VLP preparations were then dialysed against this buffer overnight at room temperature using 10 kDa molecular weight cut-off snake skin tubing (ThermoScientific) and centrifuged for at 18,000g for 10 min at 4 °C to remove any precipitates. The concentrations of purified VLPs were determined using the microplate Bradford Assay with BSA as the standard and by UV/vis spectroscopy using the calculated extinction coefficient of 1.36 mL/(mg cm) for VP1.

Dynamic Light Scattering

Dynamic light scattering (DLS) was performed using a Dynapro plate reader (Wyatt Technology, www.wyatt.com) and 384-well polystyrene plates (Corning, www.corning.com). Samples at 250 µg/mL were measured in triplicate with 10 acquisitions per well at 25 °C, and the Dynamics software (Wyatt Technology) was used for both scheduled data acquisition and analysis.

Electron Microscopy

Samples were diluted to 50 µg/mL and placed on 200-mesh carbon-coated copper grids and left to settle for 90 s. Following two washes in water, grids were negative stained with 2 % Uranyl acetate for 60 s. Transmission electron microscopy (TEM) was carried out on a JEOL 1010 at 80 kV.

Asymmetric Flow Field-Flow Fractionation

Asymmetric flow field-flow fractionation (AF4) with online multi-angle light scattering was performed by the Protein Expression Facility at the University of Queensland according to published protocols for MPyV VLPs [10].

Agarose Gel Electrophoresis

Native gels for VLP analysis comprised 1 % Tris–borate-buffered agarose. 10 % (v/v) glycerol and 0.05 % (w/v) bromophenol blue were added to 10 µg of VLPs, which were run at 8 V/cm for 90 min in 89 mM Tris–borate.

Confocal Microscopy

Confocal laser scanning microscopy was carried out using a Zeiss CLSM510 with a Zeiss Plan Apo 63× water-immersion objective. Excitation of GFP utilised the 488 nm channel of an argon ion laser, and emission from 500 to 550 nm was collected.

Results

Construct Design and Expression

To optimise translation from the wtVP1 gene in plants, we inserted the coding sequence into the transient expression vector, pEAQ-*HT* [36] containing a modified version of the CPMV RNA2 5' UTR, known as CPMV-*HT* [34], and a suppressor of post-transcriptional silencing [47]. In addition, an *N. benthamiana* codon-optimised variant (c.o.VP1) was generated that shared 77 % identity with the wtVP1 nucleotide sequence and markedly reduced variability in GC content (Supplementary Figure 1). Finally, deletion mutants were made for both native and c.o. VP1 sequences, Δ VP1, that lacked a stretch of basic residues at position 3–6 of the protein (Fig. 1b), which are in a region previously identified as a DNA binding domain and that also contributes to nuclear localisation [7, 27].

Analysis of tissue infiltrated with the various constructs by SDS-PAGE and Western blotting 5 days post-infiltra-

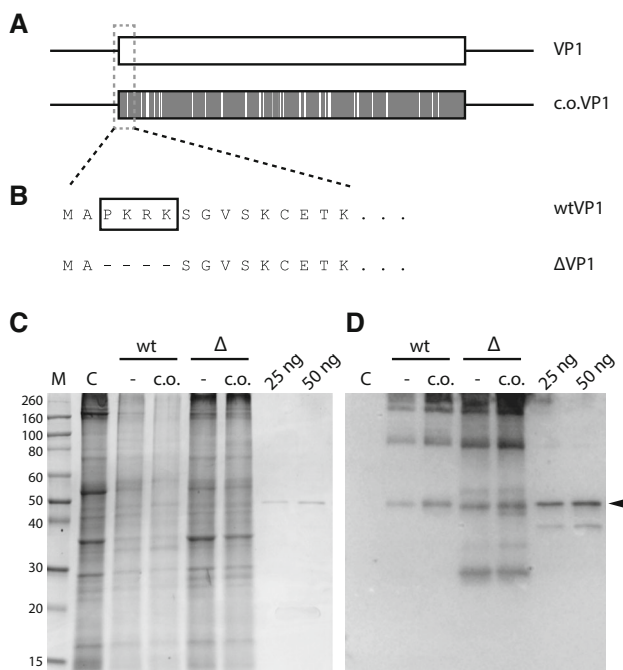


Fig. 1 Polyomavirus VP1 expression in *N. benthamiana*. **a** Schematic representation of the native (–) and codon-optimised (c.o.) VP1 sequences used for transient expression in plant leaves. **b** Amino acid sequence of the N-terminus of VP1 showing the removal of residues (boxed) to create the deletion variant Δ VP1. Extracts infiltrated with various constructs were subjected to SDS-PAGE followed by Coomassie staining (**c**) or Western blotting (**d**) with anti-VP1 serum using 25 or 50 ng of *Escherichia coli*-produced VP1 as positive control. *M* molecular weight markers with sizes indicated; *C* extract from tissue infiltrated with empty vector. The position of the VP1 monomer is shown by the arrowhead

tion (dpi) showed considerable variation between VP1 variants (Fig. 1c, d). A specific signal was detected by anti-MPyV VP1 serum compared to mock-infiltrated tissue, indicating the expression of VP1 from all constructs. A band with apparent molecular weight of approximately 45 kDa, corresponding to bacterially produced MPyV VP1, was detected for all constructs. However, leaf extracts also contained higher molecular weight species that may correspond to VP1 dimers (≈ 90 kDa) and capsomeres (≈ 212 kDa). Including these anti-VP1-specific bands showed that Δ VP1 appeared to accumulate to a much higher level than wtVP1. In addition, Δ VP1 also comprised a significant degradation product of approximately 29 kDa at this time point (Fig. 1d).

Gels are loaded on a mass basis so that comparisons can be made in terms of unit mass of fresh leaf tissue, which is more indicative of yield, and not in terms of % extracted protein. The total protein content of wtVP1-infiltrated tissue extracts was markedly lower than Δ VP1 tissue (Fig. 1c), and observation of the infiltrated leaves showed that wtVP1 expression induced necrosis, whereas Δ VP1 did not. Codon optimisation resulted in a slight improvement in expression level, particularly for wtVP1 as determined by the relative intensity of Western blot signal (Fig. 1d), and was used for all further experiments.

Consideration of the onset of necrosis led us to perform a time-course analysis of expression for codon-optimised versions of both VP1 variants to identify the optimal incubation time. Samples were taken at 2, 3, 4, 5 and 6 dpi for wtVP1 and at 2, 4, 6, 8 and 10 dpi for Δ VP1. Tissue necrosis was first observed at 4 dpi for wtVP1, which coincided with decreased VP1 expression shown by Western blot (Fig. 2a) as well as a decrease in the total protein content of the tissue. Protein concentration of extracts from wtVP1 infiltrated tissue decreased from 2.4 mg/mL at 3 dpi to 1.6 mg/mL at 4 dpi and further dropped to 0.9 and 1.1 mg/mL at 5 and 6 days, respectively. For Δ VP1-infiltrated tissue, there was no adverse effect on leaves until eventual chlorosis of infiltrated patches 10 dpi, which is commonly seen with control infiltrations. Protein content of Δ VP1 extracts was between 2.3 and 2.5 mg/mL until 10 dpi when it dropped to 1.5 mg/mL. However, Western blotting showed that the appearance of proteolytic fragments of Δ VP1 was dependent on incubation time (Fig. 2b). The previously detected fragment at 29 kDa appeared at 4 dpi and a second band approximately 36 kDa appeared after 6 dpi. These fragments continue to accumulate with incubation time as the Δ VP1 monomer level decreases, and as a result of this analysis, tissue for the purification of VLPs assembled from both VP1 variants was harvested at 3.5 dpi.

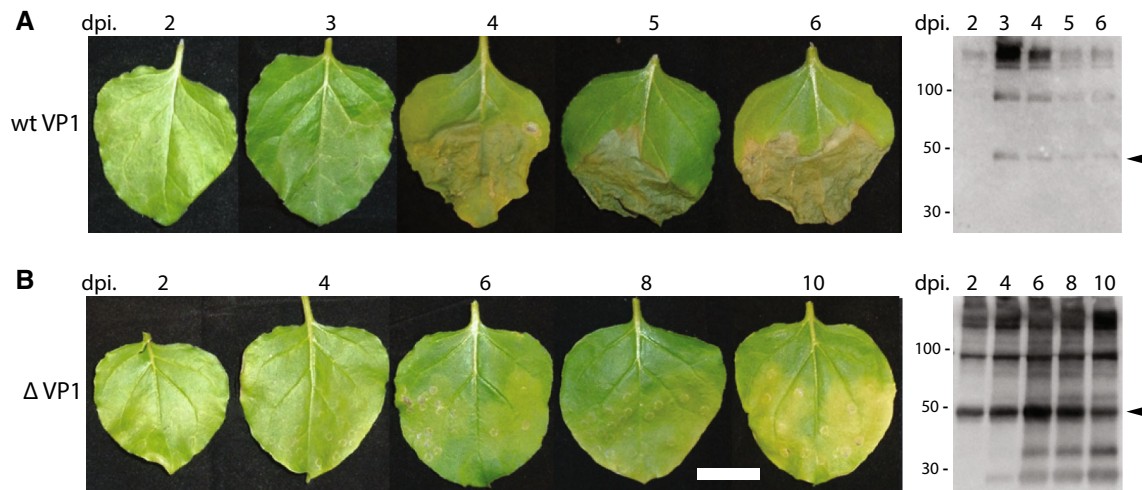


Fig. 2 Time course of VP1 expression in *N. benthamiana*. Representative leaves and anti-VP1 Western blots of extracts from tissue infiltrated with either wtVP1 (**a**) or Δ VP1 (**b**). Leaves and blots correspond to the number of days post-infiltration (d.p.i.) as shown.

The position of molecular weight markers is given to the *left* of the Western blots and the *scale bar* represents 2.5 cm for leaf images. The position of the VP1 monomer is shown by the *arrowhead*

VLP Characterisation

Single-step purification of VLPs by iodixanol density gradient resulted in the isolation of 465 μ g of wtVP1 and 648 μ g of Δ VP1 from 8 g of tissue (Supplementary Figure 2). Putative VLP samples were analysed by DLS, which indicated the presence of particles of the expected size for MPyV capsids. The wtVP1 preparation had a hydrodynamic radius (*Rh*) of 37.4 nm with a % polydispersity (Pd) of 20.3, and the Δ VP1 preparation had a *Rh* of 45.7 nm and a % Pd of 16.8, indicating monodisperse particles for this construct. TEM provided definitive evidence of VLP formation (Fig. 3). Analysis of imaged particles showed that the wtVLPs comprised a mix of three particle sizes with diameters of approximately 24, 32 and 44 nm, whereas the Δ VLPs were present as one species with a diameter of about 50 nm, in addition to the presence of what appeared to be some non-specific capsomere aggregates or disrupted VLPs. To characterise the biophysical properties of the plant-made MPyV VLPs in finer detail, field-flow fractionation coupled with multi-angle light scattering was used. AF4 identified VLP peaks with radii of 18.5 and 23 nm for wtVLPs and Δ VLPs, respectively (Fig. 4), corresponding to VLPs with average diameters of 37 nm for wtVLPs and 46 nm for Δ VLPs. The Δ VLP peak had a shoulder that may have represented non-specific aggregate or disrupted VLPs, and the wtVLP sample contained a peak eluting before the VLPs.

Plant-produced MPyV VLPs were also run on native agarose gels, which allows for the detection of encapsidated nucleic acid, as well as giving information on structural polymorphism [20]. Coomassie staining again showed a greater heterogeneity among plant-made wtVLPs than Δ VLPs and that the latter are slightly larger as they are slower

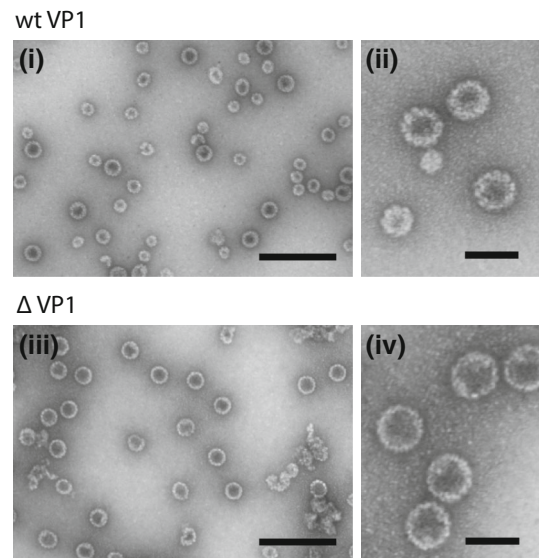


Fig. 3 Transmission electron microscopy of MPyV VLPs. TEM micrographs of uranyl acetate-stained wtVLPs (**i**, **ii**) and Δ VLPs (**iii**, **iv**). *Scale bars* represent 200 nm for **i** and **iii**, and 50 nm for **ii** and **iv**

to migrate through the gel due to their lower charge to volume ratio (Fig. 5). Staining the same gel with ethidium bromide showed that nucleic acid is encapsidated by wtVLPs with the lowest electrophoretic mobility but not more mobile wtVLPs or by Δ VLPs.

VP2C–GFP for VP1 Localisation and Foreign Protein Encapsidation

To further understand the differences between wtVLPs and Δ VLPs, we investigated the impact of the deletion on

Fig. 4 Asymmetric flow field-flow fractionation of MPyV VLPs. Overlaid AF4 fractograms of wtVLPs (*light grey*) and Δ VLPs (*dark grey*). *Solid line* represents relative absorbance at 280 nm and *open circles* indicate the root-mean-square (r.m.s.) radius

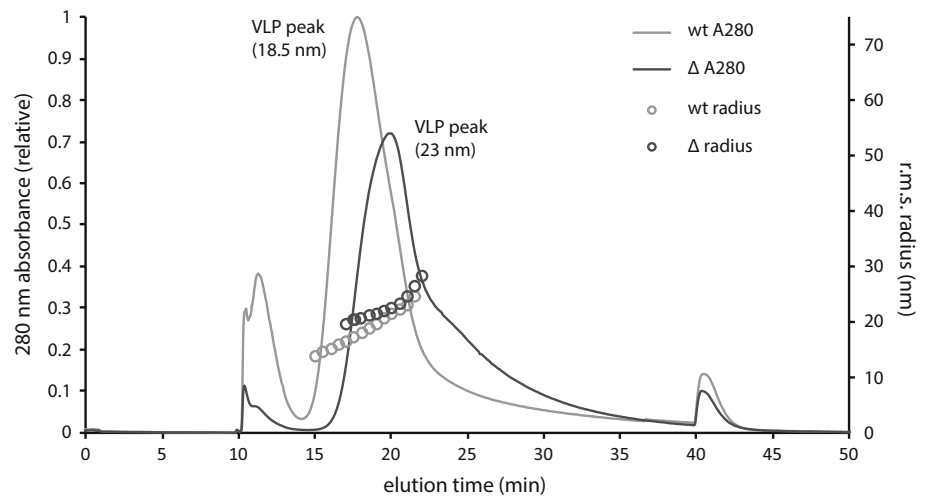
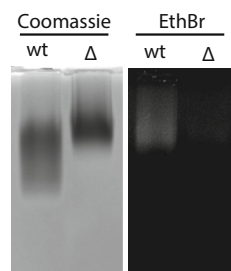


Fig. 5 Nucleic acid encapsidation by VLPs in plant leaves. Agarose gel electrophoresis of wtVLPs and Δ VLPs stained with Coomassie blue (*left*) or ethidium bromide (*right*)

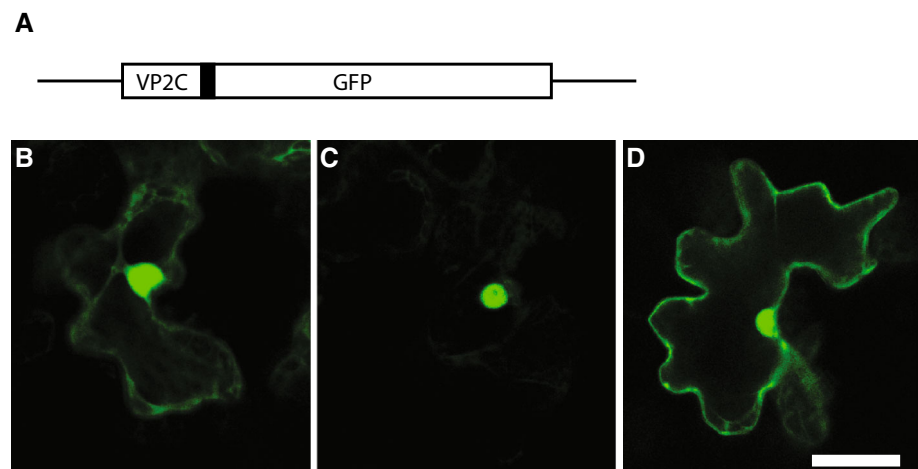


subcellular localisation of VP1 during transient expression in leaves (Fig. 6). Using the C-terminal part of MPyV VP2, known to tightly bind to the inside of MPyV capsomeres [4, 9], we constructed an *in vivo* probe for the subcellular localisation of VP1 capsomeres with GFP (Fig. 6a). The VP2C–GFP probe was infiltrated at 12.5 % of the agrobacterial optical density of VP1 constructs, and confocal microscopy showed that the fusion alone was found

in both the cytosol and the nucleus (Fig. 6a). This is expected for GFP (Fig. 6b), which passively permeates the nuclear membrane [17]. However, when the fusion was co-expressed with wtVP1, the localisation of GFP is exclusively nuclear (Fig. 6c), indicating that the VP1 NLS retains the interacting VP2C–GFP fusion in the nucleus. On the other hand, when the fusion is co-expressed with Δ VP1, exclusive nuclear localisation of GFP is lost (Fig. 6d).

To simultaneously confirm the ability of VP2C–GFP to bind to wtVP1 and Δ VP1 capsomeres and to demonstrate guest protein encapsidation in plant-made MPyV VLPs, we purified wtVLPs and Δ VLPs expressed in the presence of VP2C–GFP. The encapsidation of guest proteins into MPyV VLPs via fusion to the C-terminus of VP2, which binds to the interior cavity of capsomeres, has been demonstrated in insect cells [6] and we reasoned that *in vivo* assembly in plants would permit the same. TEM analysis of iodixanol density gradient-purified VLPs

Fig. 6 VP1 localisation in plant leaves. **a** Schematic representation of the VP2C–GFP fusion used as a probe for VP1 capsomere localisation *in vivo*. VP2C, amino acids 251–301 of MPyV VP2; *black box*, (Gly4Ser)₂ linker sequence. Confocal micrographs of leaf epidermal cells expressing VP2C–GFP alone (**b**), VP2C–GFP and wtVP1 (**c**), or VP2C–GFP and Δ VP1 (**d**). *Scale bar* represents 25 μ m



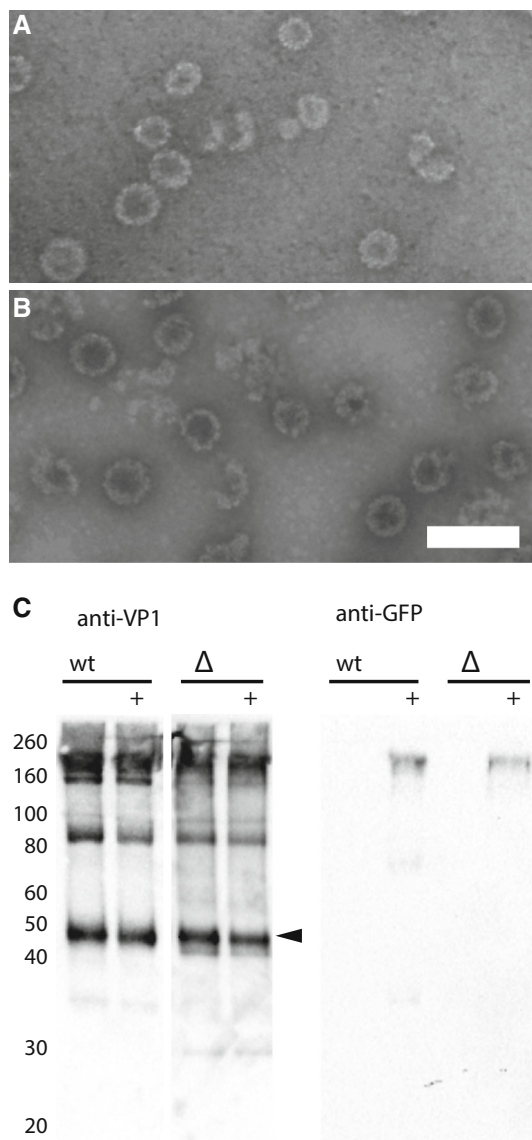


Fig. 7 Foreign protein encapsidation in plant-made MPyV VLPs. TEM micrographs of Uranyl acetate-stained wtVLPs (**a**) and Δ VLPs (**b**) co-expressed with VP2C-GFP. Scale bar represents 100 nm. **c** Anti-VP1 Western blots of wtVLPs (*left panel*) and Δ VLPs (*middle panel*) and anti-GFP Western blot (*right panel*) of purified VLPs expressed in the presence (+) or absence (–) of VP2C-GFP. The position of molecular weight markers is given to the *left* of the Western blots and the position of the VP1 monomer is shown by the *arrowhead*

showed that VLPs were indeed formed in the presence of VP2C-GFP (Fig. 7a, b). Western blot analysis of purified particles showed an anti-GFP signal specific to VLPs encapsidating GFP, which was mostly associated with VP1 complexes (Fig. 7c). The inclusion of GFP increased *Rh* of wtVLPs from 37.4 to 39.1 nm, whereas the *Rh* of Δ VLPs decreased by 2 nm and was accompanied by the appearance of some smaller particles (Fig. 7b) and an increase in Pd to 21.4 %.

Discussion

The aim of this work was to investigate the feasibility of producing polyomavirus-like particles by transient expression in plant leaves. Using a codon-optimised sequence and selecting the optimal incubation time for expression of both wtVP1 and a deletion variant, Δ VP1, we show that MPyV VLPs can be produced and purified from *N. benthamiana*. Interestingly, not only did Δ VP1 accumulate to higher levels than wtVP1, but the VLPs assembled from Δ VP1 are more uniform than wtVLPs and, unlike wtVLPs, Δ VLPs did not encapsidate nucleic acid.

Δ VLP was generated by the removal of a polybasic motif from the N-terminus of VP1. The motif is known to be involved in nuclear localisation [26], and the removal of the nuclear localisation signal from the related HPV L1 protein can improve expression of that protein in plants [23]. The present study shows that this is also the case for MPyV VP1, even though nuclear localisation was not fully excluded by Δ VP1. Early work on VP1 expression in yeast found that the first 17 amino acids of VP1 were sufficient for nuclear localisation, but that fusion to the first 12 results in nucleo-cytosolic localisation [27]. Corroborating those findings, we show that deletion of the polybasic motif within the first 12 amino acids also results in nucleo-cytosolic localisation, suggesting that the VP1 NLS is bipartite. The VP2C-GFP construct was co-infiltrated at 12.5 % of the VP1 construct optical density to ensure complete GFP-capsomere binding, and total nuclear localisation of GFP indicated that all VP2C-GFP was bound to nuclear wtVP1 capsomeres. At 33 kDa, VP2C-GFP is able to diffuse through the nuclear membrane and, as expected, is seen in both the nucleus and cytosol when expressed alone. However, capsomeres and GFP-capsomere complexes would not be able to diffuse through the nuclear membrane due to the nuclear pore size exclusion limit of around 40 kDa [24]. Therefore, the localisation of GFP fluorescence is a strong indication of active capsomere localisation. However, we cannot rule out the possibility that when co-expressed with Δ VP1, some unbound GFP freely diffuses through the nuclear membrane.

The VP1 DNA binding site is also located within the first 6 amino acids of the VP1 amino terminus [26] and is not sequence specific [7]. Therefore, another advantage of removing this motif is the avoidance of cellular DNA packaging. Indeed, we found that wtVLPs contained DNA, whereas Δ VLPs did not, which is in agreement with previous findings in insect cells [15]. This is a significant benefit in biotechnology as undefined nucleic acid encapsidation is seen as a contaminant in the case of vaccines and having an empty capsid enables the directed encapsidation of therapeutics and

diagnostics [2, 48, 50]. Moreover, it seems likely that the elimination of DNA binding also obviated the necrotising effect of wtVP1 on leaf tissue.

Detailed biophysical characterisation showed a considerable difference between wtVLPs and Δ VLPs. TEM revealed heterogeneity in the size of wtVLPs, and in terms of the % Pd as measured by DLS, the preparation would be considered polydisperse. Unless they are purified from MPyV infections or assembled under precisely defined conditions, particle size variation is a feature of MPyV VLPs, and discrete particles with diameter of 50, 32 and 26 nm have previously been identified by TEM [38]. On the other hand, the Δ VP1 modification resulted in monodisperse VLPs of a slightly larger radius than wtVLPs, more similar to native virions [37]. The N-terminal arm of VP1 forms a clamp to hold C-terminal protrusions from neighbouring capsomeres in place [44], and recent structural evidence suggests the presence of intercapsomeric disulphide bridges linking the N-termini of VP1 from different capsomeres [43]. Flexibility in this clamping mechanism allows capsomeres to exist in both pentavalent and hexavalent states [31, 37] as well as tolerating the assembly of polymorphic particles in the polyomaviruses [28, 38]. It is possible that the N-terminal modification of Δ VP1 affects intercapsomeric interactions such that they cannot efficiently accommodate the higher curvature needed to form smaller particles. While the encapsidation of foreign proteins has been shown to slightly increase the radius of wtVLPs [19], it is surprising to note that the inclusion of VP2C–GFP can result in the formation of smaller Δ VLPs, though the mechanism by which this occurs requires further investigation.

The yield of purified VLPs was 58 μ g/(g fresh weight tissue) for wtVLPs and 81 μ g/(g fresh weight tissue) for Δ VLPs. This suggests that the apparent dimers and higher molecular weight species identified by Coomassie staining and detected by anti-VP1 antibodies did indeed indicate additional VP1 protein, which contributed to the final yield (see Supplementary Figure 2). Throughout this study, plant-expressed VP1 was recalcitrant to reduction by either DTT or β -mercaptoethanol (data not shown). Dimers and higher order VP1 aggregates have been seen on reducing SDS-PAGE gels from purified virions [13] and recombinant VP1 expressed in insect cells [15]. It is expected that both intracapsomeric and intercapsomeric disulphide bridges are more efficiently formed during *in vivo* assembly than *in vitro* and this results in VLPs from eukaryotic cells possessing greater stability than *in vitro*-assembled VLPs [43]. Despite limited optimisation performed during this study and the analysis of just two gradient fractions, the recovery of purified VLPs approaches the highest reported levels of HPV L1 protein in crude extracts of plant tissue [21, 23]. Purification could certainly be optimised with improved

gradient and ultracentrifugation conditions, which could also benefit from a pre-enrichment of VLPs by, for example, PEG precipitation [14]. In addition, steps could be taken to improve the upstream process for plant-produced polyomavirus-like particles.

As the band pattern detected by anti-VP1 antibodies was not affected by codon optimisation, the degradation of Δ VP1 is most likely due to proteolysis rather than an mRNA degradation effect. MPyV VP1 has long been known to yield a 29 kDa proteolytic fragment [13] and is susceptible to cleavage by S1 serine proteases [11]. Interestingly, wtVP1 was not susceptible to degradation, which suggests that proteolysis occurred in the cytosol. Proteolysis can often be a limiting factor for expression in plant cells [5], and it may be possible to address this issue through a number of strategies. For example, the stable or transient co-expression of serine protease inhibitors as has been demonstrated for aspartic proteases in the cytosol [16] and cysteine proteases in the secretory pathway [33], or by post-transcriptionally regulating endogenous protease levels as recently demonstrated with anti-sense RNA inhibition [22].

To our knowledge, this study represents the first example of a polyomavirus-like particle to be expressed and purified from plant tissue. Excellent yields were obtained using a single purification step, and the VLPs were shown to be consistent with those produced in other expression hosts or assembled *in vitro*. In addition, VLPs generated from a variant of VP1 differed from wtVLPs in a number of important ways; Δ VLPs were larger and more homogenous than wtVLPs and they did not encapsidate nucleic acid. These attributes make plant-derived polyomavirus VLPs attractive for further development in biotechnology and nanotechnology, where consistent size and shape as well as the absence of contaminating nucleic acid are advantageous. Likewise, the elimination of nucleic acid binding sequences from VP1 could be used to improve homogeneity and avoid nucleic acid encapsidation in other expression hosts where nucleic acid contamination, or particle heterogeneity, is problematic. Furthermore, we show that transient expression in plants provides a facile technique for the production of VLPs loaded with encapsidated foreign proteins. The detailed characterisation of loaded MPyV VLPs and their potential application is the subject of further experimentation. In summary, this work demonstrates the potential for plant-based expression in the future of polyomavirus-like particles in vaccine development and other biotechnological applications.

Acknowledgments The authors would like to thank Dr. Alexandra Depelsenaire for assistance with confocal microscopy. Professor George Lomonosoff and Plant Biosciences Limited are thanked for providing the pEAQ-HT plasmid.

References

- Abbing, A., Blaschke, U. K., Grein, S., Kretschmar, M., Stark, C. M., Thies, M. J., et al. (2004). Efficient intracellular delivery of a protein and a low molecular weight substance via recombinant polyomavirus-like particles. *The Journal of Biological Chemistry*, 279, 27410–27421.
- Aljabali, A. A., Sainsbury, F., Lomonosoff, G. P., & Evans, D. J. (2010). Cowpea mosaic virus unmodified empty viruslike particles loaded with metal and metal oxide. *Small (Weinheim an der Bergstrasse, Germany)*, 6, 818–821.
- Anggraeni, M. R., Connors, N. K., Wu, Y., Chuan, Y. P., Lua, L. H. L., & Middelberg, A. P. J. (2013). Sensitivity of immune response quality to influenza helix 190 antigen structure displayed on a modular virus-like particle. *Vaccine*, 31, 4428–4435.
- Barouch, D. H., & Harrison, S. C. (1994). Interactions among the major and minor coat proteins of polyomavirus. *Journal of Virology*, 68, 3982–3989.
- Benchabane, M., Goulet, C., Rivard, D., Faye, L., Gomord, V., & Michaud, D. (2008). Preventing unintended proteolysis in plant protein biofactories. *Plant Biotechnology Journal*, 6, 633–648.
- Boura, E., Liebl, D., Spisek, R., Fric, J., Marek, M., Stokrova, J., et al. (2005). Polyomavirus EGFP-pseudocapsids: Analysis of model particles for introduction of proteins and peptides into mammalian cells. *FEBS Letters*, 579, 6549–6558.
- Chang, D., Cai, X., & Consigli, R. A. (1993). Characterization of the DNA binding properties of polyomavirus capsid protein. *Journal of Virology*, 67, 6327–6331.
- Chen, Q., & Lai, H. (2013). Plant-derived virus-like particles as vaccines. *Human Vaccines and Immunotherapy*, 9, 26–49.
- Chen, X. S., Stehle, T., & Harrison, S. C. (1998). Interaction of polyomavirus internal protein VP2 with the major capsid protein VP1 and implications for participation of VP2 in viral entry. *The EMBO Journal*, 17, 3233–3240.
- Chuan, Y. P., Fan, Y. Y., Lua, L., & Middelberg, A. P. J. (2008). Quantitative analysis of virus-like particle size and distribution by field-flow fractionation. *Biotechnology and Bioengineering*, 99, 1425–1433.
- Connors, N. K., Wu, Y., Lua, L. H. L., & Middelberg, A. P. J. (2014). Improved fusion tag cleavage strategies in the downstream processing of self-assembling virus-like particle vaccines. *Food and Bioprocess Processing*, 92, 143–151.
- DeCaprio, J. A., & Garcea, R. L. (2013). A cornucopia of human polyomaviruses. *Nature Reviews Microbiology*, 11, 264–276.
- Friedmann, T. (1976). Structural proteins of polyoma virus: Proteolytic degradation of virion proteins by exogenous and by virion-associated proteases. *Journal of Virology*, 20, 520–526.
- Friedmann, T., & Haas, M. (1970). Rapid concentration and purification of polyoma virus and SV40 with polyethylene glycol. *Virology*, 42, 248–250.
- Gillock, E., & Consigli, R. (1998). Truncation of the nuclear localization signal of polyomavirus VP1 results in a loss of DNA packaging when expressed in the baculovirus system. *Virus Research*, 58, 149–160.
- Goulet, C., Khalf, M., Sainsbury, F., D'Aoust, M. A., & Michaud, D. (2012). A protease activity-depleted environment for heterologous proteins migrating towards the leaf cell apoplast. *Plant Biotechnology Journal*, 10, 83–94.
- Grebenok, R. J., Pierson, E., Lambert, G. M., Gong, F. C., Afonso, C. L., Haldeman-Cahill, R., et al. (1997). Green-fluorescent protein fusions for efficient characterization of nuclear targeting. *The Plant Journal*, 11, 573–586.
- Leavitt, A. D., Roberts, T. M., & Garcea, R. L. (1985). Polyoma virus major capsid protein, VP1. Purification after high level expression in *Escherichia coli*. *The Journal of Biological Chemistry*, 260, 12803–12809.
- Lipin, D. I., Chuan, Y. P., Lua, L. H. L., & Middelberg, A. P. J. (2008). Encapsulation of DNA and non-viral protein changes the structure of murine polyomavirus virus-like particles. *Archives of Virology*, 153, 2027–2039.
- Lua, L. H. L., Connors, N. K., Sainsbury, F., Chuan, Y. P., Wibowo, N., & Middelberg, A. P. J. (2014). Bioengineering virus-like particles as vaccines. *Biotechnology and Bioengineering*, 111, 425–440.
- Maclean, J., Koekemoer, M., Olivier, A. J., Stewart, D., Hitzeroth, I. I., Rademacher, T., et al. (2007). Optimization of human papillomavirus type 16 (HPV-16) L1 expression in plants: Comparison of the suitability of different HPV-16 L1 gene variants and different cell-compartment localization. *Journal of General Virology*, 88, 1460–1469.
- Mandal, M. K., Fischer, R., Schillberg, S., & Schiermeyer, A. (2014). Inhibition of protease activity by antisense RNA improves recombinant protein production in *Nicotiana tabacum* cv. Bright yellow 2 (BY-2) suspension cells. *Biotechnology Journal*, 9, 1065–1073.
- Matic, S., Masenga, V., Poli, A., Rinaldi, R., Milne, R. G., Vecchiati, M., & Noris, E. (2012). Comparative analysis of recombinant human papillomavirus 8 L1 production in plants by a variety of expression systems and purification methods. *Plant Biotechnology Journal*, 10, 410–421.
- Merkle, T. (2003). Nucleo-cytoplasmic partitioning of proteins in plants: Implications for the regulation of environmental and developmental signalling. *Current Genetics*, 44, 231–260.
- Middelberg, A. P., Rivera-Hernandez, T., Wibowo, N., Lua, L. H., Fan, Y., Magor, G., et al. (2011). A microbial platform for rapid and low-cost virus-like particle and capsomere vaccines. *Vaccine*, 29, 7154–7162.
- Moreland, R., Montross, L., & Garcea, R. (1991). Characterization of the DNA-binding properties of the polyomavirus capsid protein VP1. *Journal of Virology*, 65, 1168–1176.
- Moreland, R. B., & Garcea, R. L. (1991). Characterization of a nuclear localization sequence in the polyomavirus capsid protein VP1. *Virology*, 185, 513–518.
- Nilsson, J., Miyazaki, N., Xing, L., Wu, B., Hammar, L., Li, T. C., et al. (2005). Structure and assembly of a T = 1 virus-like particle in BK polyomavirus. *Journal of Virology*, 79, 5337–5345.
- Pastrana, D. V., Brennan, D. C., Cuburu, N., Storch, G. A., Viscidi, R. P., Randhawa, P. S., & Buck, C. B. (2012). Neutralization serotyping of BK polyomavirus infection in kidney transplant recipients. *PLoS Pathogens*, 8, e1002650.
- Paul, M., & Ma, J. K. (2011). Plant-made pharmaceuticals: Leading products and production platforms. *Biotechnology and Applied Biochemistry*, 58, 58–67.
- Rayment, I., Baker, T. S., Caspar, D. L., & Murakami, W. T. (1982). Polyoma virus capsid structure at 22.5 Å resolution. *Nature*, 295, 110–115.
- Rivera-Hernandez, T., Hartas, J., Wu, Y., Chuan, Y. P., Lua, L. H., Good, M., et al. (2013). Self-adjuvanting modular virus-like particles for mucosal vaccination against group A streptococcus (GAS). *Vaccines*, 31, 1950–1955.
- Robert, S., Khalf, M., Goulet, M. C., D'Aoust, M. A., Sainsbury, F., & Michaud, D. (2013). Protection of recombinant mammalian antibodies from development-dependent proteolysis in leaves of *Nicotiana benthamiana*. *PLoS One*, 8, e70203.
- Sainsbury, F., & Lomonosoff, G. P. (2008). Extremely high-level and rapid transient protein production in plants without the use of viral replication. *Plant Physiology*, 148, 1212–1218.

35. Sainsbury, F., & Lomonosoff, G. P. (2014). Transient expressions of synthetic biology in plants. *Current Opinion in Plant Biology*, *19*, 1–7.
36. Sainsbury, F., Thuenemann, E. C., & Lomonosoff, G. P. (2009). pEAQ: Versatile expression vectors for easy and quick transient expression of heterologous proteins in plants. *Plant Biotechnology Journal*, *7*, 682–693.
37. Salunke, D. M., Caspar, D. L., & Garcea, R. L. (1986). Self-assembly of purified polyomavirus capsid protein VP1. *Cell*, *46*, 895–904.
38. Salunke, D. M., Caspar, D. L., & Garcea, R. L. (1989). Polymorphism in the assembly of polyomavirus capsid protein VP1. *Biophysical Journal*, *56*, 887–900.
39. Sasnauskas, K., Bulavaite, A., Hale, A., Jin, L., Knowles, W. A., Gedvilaite, A., et al. (2002). Generation of recombinant virus-like particles of human and non-human polyomaviruses in yeast *Saccharomyces cerevisiae*. *Intervirology*, *45*, 308–317.
40. Sasnauskas, K., Buzaitė, O., Vogel, F., Jandrig, B., Razanskas, R., Staniulis, J., et al. (1999). Yeast cells allow high-level expression and formation of polyomavirus-like particles. *Biological Chemistry*, *380*, 381–386.
41. Schumacher, T., Ruehland, C., Schultheiss, C., Brinkman, M., Roedel, F., Reiser, C. O., et al. (2007). Advanced antigen delivery of murine survivin: Chimeric virus-like particles in cancer vaccine research. *International Journal of Biomedical Science: IJBS*, *3*, 199–205.
42. Scotti, N., & Rybicki, E. (2013). Virus-like particles produced in plants as potential vaccines. *Expert Reviews Vaccines*, *12*, 211–224.
43. Simon, C., Klose, T., Herbst, S., Han, B. G., Sinz, A., Glaeser, R. M., et al. (2014). Disulfide linkage and structure of highly stable yeast-derived virus-like particles of murine polyomavirus. *The Journal of Biological Chemistry*, *289*, 10411–10418.
44. Stehle, T., & Harrison, S. (1996). Crystal structures of murine polyomavirus in complex with straight-chain and branched-chain sialyloligosaccharide receptor fragments. *Structure*, *4*, 183–194.
45. Tegerstedt, K., Lindencrona, J., Curcio, C., Andreasson, K., Tullus, C., Forni, G., et al. (2005). A single vaccination with polyomavirus VP1/VP2Her2 virus-like particles prevents outgrowth of Her-2/neu-expressing tumors. *Cancer Research*, *65*, 5953–5957.
46. Teunissen, E. A., de Raad, M., & Mastrobattista, E. (2013). Production and biomedical applications of virus-like particles derived from polyomaviruses. *Journal of Controlled Release*, *172*, 305–321.
47. Voinnet, O., Rivas, S., Mestre, P., & Baulcombe, D. (2003). An enhanced transient expression system in plants based on suppression of gene silencing by the p19 protein of tomato bushy stunt virus. *The Plant Journal*, *33*, 949–956.
48. Wen, A. M., Shukla, S., Saxena, P., Aljabali, A. A., Yildiz, I., Dey, S., et al. (2012). Interior engineering of a viral nanoparticle and its tumor homing properties. *Biomacromolecules*, *13*, 3990–4001.
49. White, M. K., Gordon, J., & Khalili, K. (2013). The rapidly expanding family of human polyomaviruses: Recent developments in understanding their life cycle and role in human pathology. *PLoS Pathogens*, *9*, e1003206.
50. Wu, W., Hsiao, S. C., Carrico, Z. M., & Francis, M. B. (2009). Genome-free viral capsids as multivalent carriers for taxol delivery. *Angewandte Chemie*, *48*, 9493–9497.